Turkish Computational and Theoretical Chemistry

Turkish Comp Theo Chem (TC&TC)

Volume(Issue): 5(2) – Year: 2021 – Pages: 24-34

e-ISSN: 2602-3237

https://doi.org/10.33435/tcandtc. 926405

Received: 22.04.2021 ***Accepted:*** 04.06.2021 *Research Article*

DFT/TDDFT studies of the structural, electronic, NBO and non-linear optical proper-ties of triphenylamine functionalized tetrathiafulvalene

Ahmed Azaid[a], Tayeb Abram[a], Rchid Kacimi[a], Marzouk Raftani[a], Chebil Samaher[b], Abdelouahid Sbai[a], Tahar Lakhlifi[a], Mohammed Bouachrine[1,a,c]

[a]Molecular Chemistry and Natural Substances Laboratory, Faculty of Sciences, University Moulay Ismail, Meknes, Morocco

[b]Synthèse asymétriques Et ingénierie moléculaires des matériaux Nouveaux Pour L'électronique Organique (LR 18ES19) Faculté des Sciences de Monastir, Université de Monastir-Tunisie, Monastir, Tunisia

[c]EST Khenifra, University Sultan Moulay Sliman, Morocco

Abstract:

In this paper, we present a theoretical analysis of the molecular structure of a conjugated molecule TTPA-TTF at the DFT level using the B3LYP method and the 6-31G (d) basis set. The TTPA-TTF mole-cule presented a twisted configuration, which gave it good solubility in different organic solvents. The Partial atomic charge, molecular electrostatic potential (MEP) map, and global reactivity descriptors highlight the reactive sites of the molecule with the possible prediction of its reactivity. Moreover, a clear image of the intra- and intermolecular interactions illustrates hyperconjugative interactions based on the charge delocalization that emerges from the natural bond orbital analysis. The non-linear optical proper-ties of the TTPA-TTF molecule can also be calculated by determining their first hyperpolarizabilities. The time-dependent density theory method TD-DFT-B3LYP 6-31G (d) was used for the study of absorption. The obtained results show a broad spectrum in the visible range favorable to harvest solar light.

Keywords: *Tetrathiafulvalene, Triphenylamine, DFT, TD-DFT, NLO, NBO and APT*

1. Introduction

Following the discovery in 1973 of TTF-first TCNQ's metallic load transfer salt [1], detailed research have concentrated on the design and synthesis of tetrathiafulvalene (TTF) derivatives [2-3-4]. Tetrathiafulvalene (TTF) is rare among organic molecules in that it is characterized by a simple structure and is associated with a variety of applications [5-6-7]. Due to its good electron-donating capability and synthesis nearly forty years ago, the development and synthesis of tetrathiafulvalene (TTF) derivatives have been the subject of several studies [8]. These capabili-ties importantly allow useful applications in the chemistry of materials [5], conductors [9] and superconductors [10], adducts with C60 [11], conductive polymers [12], materials for non-linear optics (NLO) [13], cationic sponges [14], ferromagnetic organic magnets [15], liquid crys-tals [16], dendrimers [17], molecular rotaxanes and catenanes[18].

TTF has also played an important role in su-pramolecular chemistry and the creation of me-chanically inter-locked molecules, electrochromic materials, molecular switches, and devices, where flexibility can be integrated due to TTF deriva-tives electron donor capacity and ability to form donor-acceptor complexes with electron accep-tors [19].

In this context, TTF derivatives functional-ized with peripheral groups should be developed for the next use, particularly for those containing heteroatoms. Recently, a study based on synthe-sis

[1] Corresponding Authors

e-mail: m.bouachrine@umi.ac.ma

and properties of triphenylamine functional-ized tetrathiafulvalene has been carried out by Xia Tian et al [20]. The TTPA-TTF compound characterized by an p-conjugation system, has excellent electronic donating ability and hole-transporting capability, as well as three-dimensional molecular structures [21-22-23].

The chemical structure of the studied com-pound studied is shown in Figure 1. This article focuses primarily on a full explanation of the geometrical parameters, the optical and electron-ic properties, the ionization potentials (IP), the electron affinities (EA), chemical reactivity indi-ces, the molecular electrostatic potential (MEP), and the non-linear optical parameters (NLO). Furthermore, the charge transfer properties and polarization were estimated using the atomic polarizability tensor (APT) charges. Finally, the natural bond orbital (NBO) approach was used to examine the molecule's stability as a result of hyper-conjugative interaction and charge delo-calization.

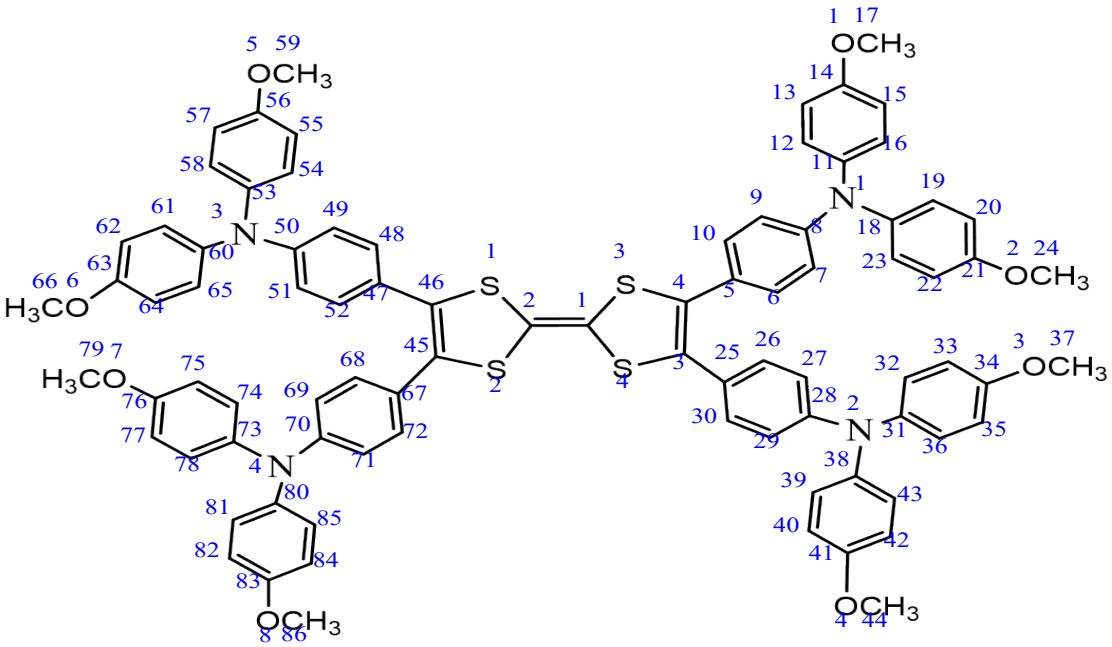

Figure 1. Molecular structures of TTPA-TTF

2. Computational Method

In this work, DFT method with the B3LYP functional Becke's three-parameter non-local exchange functional with the Lee-Yang–Parr correlation function) [24] and Pople's basis set 6-31G(d) [20] has been used in all the study of the neutral compound in the gaseous state. It is noted that all of these calculations have been per-formed using the Gaussian 09 package [25]. The abortion properties of the molecule TTPA-TTF are calculated using Time-Dependent Density Functional Theory (TD-DFT (B3LYP)) method. The associated HOMO and LUMO energies were then used to theoretically calculate certain overall parameters of chemical reactivity such as elec-tronegativity (χ), chemical potential (μ), electro-philicity index (ω) and chemical hardness (η) and softness (S) [26-27-28]. In addition, the APT partial charges, the dipole moment of the mole-cule TTPA-TTF and the molecular electrostatic potential (MEP) map, were performed using the same functionals. Finally, the natural bond or-bital (NBO) and NLO properties of specific struc-tures investigation was performed using the same functionals for the approximation of charge transfer interactions of investigated compound.

3. Results and discussion

3.1. Geometrical parameters

To determine the geometrical parameters, the TTPA-TTF molecule is fully optimized at the B3LYP/ 6-31G(d) [29] level of theory in the gas phase. The general chemical structure of the studied compound is presented in figure 2 and its parameters are collected in Table 1 and Figure 3.

The link distance parameters di (i = 1– 4) show that the corresponding binding distances in TTPA-TTF compose are similar (d =1.47 Å). while the dihedral angles θi (i = 1–4) between the oriented TTF and the peripheral TPA groups for TTPA-

TTF were in the range of 45°- 47°, suggest-ing that the compound had a twisted structure. Moreover, the centered tetrathiafulvalene (TTF) unit has a structure planar p-conjugate.

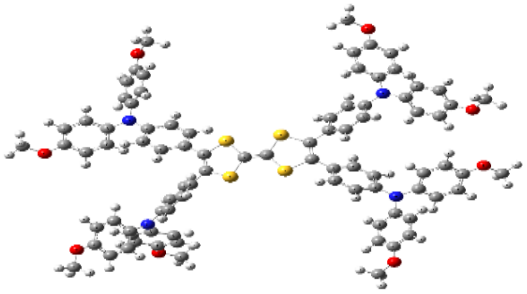

Figure 2. Optimized structures of the molecule TTPA-TTF

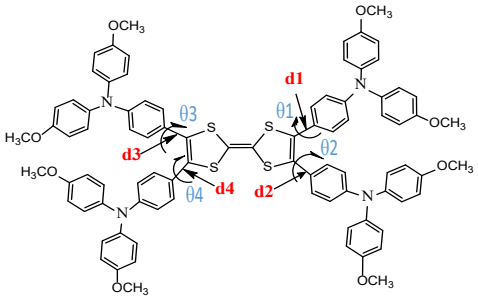

Figure 3. Chemical structure of the molecule TTPA-TTF

Table 1. Inter-ring bond lengths di and dihedral angles θi of TTPA-TTF

	d1	d2	d3	d4
TTPA-TTF	1.47	1.47	1.47	1.47
	θ2	θ2	θ2	θ2
	45.83	48.05	-46.34	-44.30

3.2. Atomic charges (APT)

The Atomic Polar Tensor (APT) was used to measure the atomic charges in TTPA-TTF. This tensor can be based on the total of the charge and charge-flux tensors [30]. Table 2 and figure 1 illustrate the atomic charges associated with TTPA-TTF. Atomic charge simulations are important in quantum mechanical studies of molecular systems since they are used to illustrate molecular dipole moments, polarizabilities, electronic structures and hence chemical reactivities. According to the atomic charge study of TTPA-TTF, the components of APT calculated of the four sulfur atoms of tetrathiafulvalene unit var-ies from -0.33 e to -0.36 e. The four nitrogen atoms in the triphenylamine units have the larg-est negative charge values such as -1.26 e and -1.24 e.

The eight oxygen atoms are also negatively charged with values -1.02 e to -1.07 e. The C(1), C(2), C(3), C(4), C(45) and C(46) atoms of the tetrathiafulvalene unit are all positive, with val-ues varying from 0.15 e to 0.32 e. The carbon atoms of the triphenylamine fragments change the sign from -0.02 e to 0.84 e.

3.3. Molecular electrostatic potential

The MEP is a good descriptor for detecting sites for electrophilic and nucleophilic attack reactions, as well as hydrogen bonding interac-tions, it is directly related to electron density [31-32]. All chemical system creates an electrostatic potential in all directions. According to the MESP map, negative and positive potentials are repre-sented by red and blue regions, which correspond respectively to the region rich in electrons and deficient in electrons, whereas the neutral electrostatic potential is indicated by green color [33]. The molecular electrostatic potential was estimated using the B3LYP /6-31G (d) method (Figure 4).

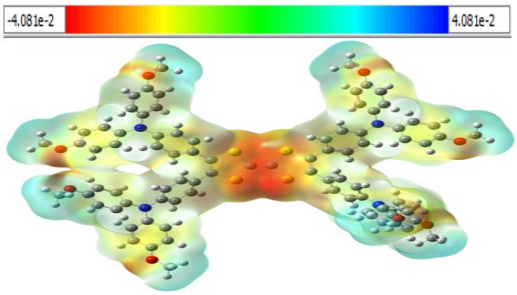

Figure 4. Molecular electrostatic potential map of TTPA-TTF.

The determined limits are -4.081e^{-2} (deepest red) and +4.081e^{-2} (deepest blue), with the intermediate scale of colors changing from red to orange, yellow, green, and blue in order, as shown in Figure 4. Indeed, the most negative potential is focused around the TTF unit and oxygen atoms, while the methoxyphenyl H atoms have a more positive potential.

3.4. Front molecular orbitals and HOMO–LUMO gaps

To have a good understanding of the excitation characteristics and ICT of π-conjugated systems, it is necessary to investigate the HOMO and LUMO of our molecule [34]. As a result, the HOMO and LUMO orbitals of the TTPA-TTF molecule have been calculated from the optimized structure using

the DFT/B3LYP/6-31G (d) method. The frontier molecular orbitals (FMO) for this compound are displayed in Figure 5. The relative order of HOMO and LUMO orbitals provides a reasonable qualitative indication of the excitation proper-ties as well as other properties such as optical properties [35]. As anticipated, the electron distributions of the highest occupied molecular orbital (HOMO) of TTPA-TTF was mainly localized on the TTF center, the electron distributions of the highest occupied molecular orbital (HOMO) of TTPA-TTF was mainly localized on the TTF center, while the lowest unoccupied molecular orbital (LUMO) just slightly shifted from TTF unit to the adjacent phenyl rings. This result indicates the donor character of the molecule is mainly stems from the TTF. Moreover, the calculated energy band gap (Egap = ELUMO - EHOMO) is equal to 3.055 eV.

3.5. UV–Vis spectral analysis

To understand the electronic transitions of TTPA-TTF molecule and to simulate the theoretical electron absorption spectrum, we performed calculations using the TD-DFT/ B3LYP [36] quantum chemistry method with the Pople 6-31G (d) basis sets [37]. The parameters considered are as follows: The vertical excitation energy (Eex), the wave-length of absorption (λmax) and oscillator forces (f). The numerical results are summarized in table 3, while figure 6 shows the simulated spectra. The results in Table 3 and figure 6 show that the maximum absorption wavelength of TTPA-TTF is 431.321 nm, which can be attributed to a more localized p-p* in peripheral TPA rings and centered TTF. In addition, this value indicates its high transparency to visible light. Indeed, the transition from the ground state to the first excited state (S0→S1) at 431.321nm corresponds to the transition from HOMO to LUMO with a contribution of 10%. The next transition corresponds to the HOMO→LUMO+6 transition with a contribution of 9%. Indeed, the most intense transition corresponding to the most important oscillator force (0.1507), it is about a HOMO→LUMO+2 transition with a contribution of 74%.

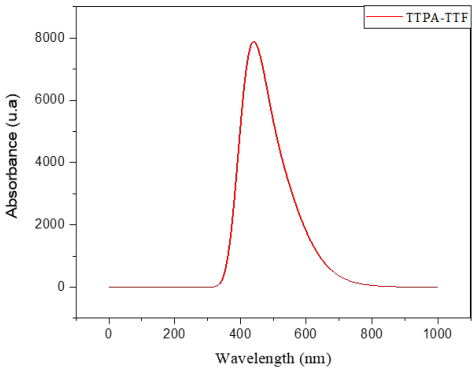

Figure 6. Simulated UV–visible optical absorption spectra of TTPA-TTF obtained by using TD-DFT/B3LYP/6-31G (d)

3.6. Global reactivity descriptors

To explain or predict the reactivity of molecular systems, Certain terms in chemistry have been developed such as ionization potential (I), electron affinity (A), chemical potential (μ), chemical hardness (η), electronegativity (χ), chemical softness (S) and electrophilicity (ω). These global reactivity descriptors were investigated using TTPA-TTF optimization in the gas phase. The numerical reactivity descriptors, which are primarily based on HOMO and LUMO levels of studied compounds, are summarized in Table 4. According to the Koopmans theorem, the ionization potential (I) and electron affinity (A) can be defined by the equations (1) and (2) [38] and according to Parr [39], we calculated the different chemical parameters, namely the electronic chemical potential (μ), electronegativity (χ), and global hardness (η) using equations (3), (4) and (5) respectively [39-40]. Electrophilicity index (ω) and the global chemical softness (S) are defined as follows (equations (6) and (7))

$$I = -E_{HOMO} \quad (1)$$

$$A = -E_{LUMO} \quad (2)$$

$$\mu = \frac{E_{LUMO} + E_{HOMO}}{2} \quad (3)$$

$$\chi = -\mu \quad (4)$$

$$\eta = \frac{E_{LUMO} - E_{HOMO}}{2} \quad (5)$$

$$\omega = \frac{\mu^2}{2\eta} \quad (6)$$

$$S = \frac{1}{\eta} \quad (7)$$

Table 2. Atomic charges of the optimized TTPA-TTF molecule

Atom	Charge	Atom	Charge	Atom	Charge
S(1)	-0.33	C(19)	-0.25	C(53)	0.42
S(2)	-0.35	C(20)	-0.12	C(54)	-0.05
S(3)	-0.33	C(21)	0.64	C(55)	-0.12
S(4)	-0.36	C(22)	-0.10	C(56)	0.66
N(1)	-1 .26	C(23)	-0.02	C(57)	-0.09
N(2)	-1.26	C(24)	0.61	C(58)	-0.03
N(3)	-1.24	C(25)	-0.10	C(59)	0.57
N(4)	-1.24	C(26)	0.10	C(60)	0.37
O(1)	-1.03	C(27)	-0.23	C(61)	-0.02
O(2)	-1.03	C(28)	0.84	C(62)	-0.11
O(3)	-1.02	C(29)	-0.24	C(63)	0.62
O(4)	-1.07	C(30)	0.06	C(64)	-0.10
O(5)	-1.04	C(31)	0.42	C(65)	-0.03
O(6)	-1.03	C(32)	-0.02	C(66)	0.62
O(7)	-1.02	C(33)	-0.10	C(67)	-0.10
O(8)	-1.05	C(34)	0.67	C(68)	0.06
C(1)	0 .15	C(35)	-0.12	C(69)	-0.25
C(2)	0.15	C(36)	-0.03	C(70)	0.78
C(3)	0.27	C(37)	0.61	C(71)	-0.22
C(4)	0.32	C(38)	0.37	C(72)	0.10
C(5)	-0.15	C(39)	-0.02	C(73)	0.36
C(6)	0.10	C(40)	-0.09	C(74)	-0.03
C(7)	-0.27	C(41)	0.65	C(75)	-0.10
C(8)	0.8	C(42)	-0.12	C(76)	0.63
C(9)	0.26	C(43)	-0.03	C(77)	-0.11
C(10)	0.13	C(44)	0.56	C(78)	-0.02
C(11)	0.47	C(45)	0.27	C(79)	0.61
C(12)	-0.04	C(46)	0.31	C(80)	0.48
C(13)	0.17	C(47)	-0.14	C(81)	-0.03
C(14)	0.66	C(48)	0.12	C(82)	-0.09
C(15)	-0.10	C(49)	-0.24	C(83)	0.67
C(16)	-0.02	C(50)	0.08	C(84)	-0.12
C(17)	0.57	C(51)	-0.26	C(85)	-0.05
C(18)	0.38	C(52)	0.09	C(86)	0.57

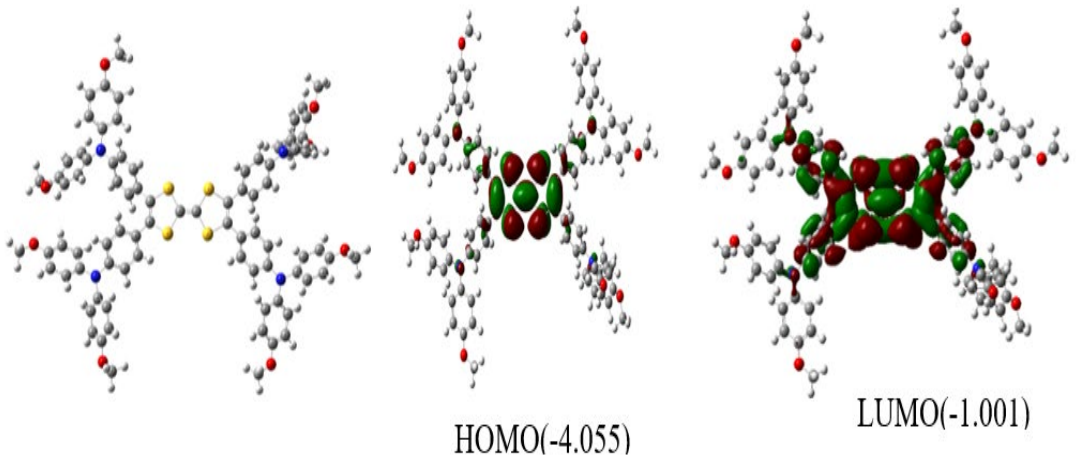

Figure 5. The contour plots of HOMO and LUMO orbitals of the TTPA-TTF.

Table 3. Absorption properties obtained by TD-DFT method for TTPA-TTF

	λ (nm)	λ_{exp} (nm)[a]	Energy (eV)	f	MO/character
TTPA-TTF	431.321	$300 < \lambda_{exp} < 400$	2.87	0.150	HOMO->LUMO (10%) HOMO->L+6 (9%) HOMO -> L+2 (74%)

[a]Experimental values in parentheses are from Ref.[20].

The ionization potential (I) is characterized as the energy needed to remove one electron from a molecule in its molecular environment. The high energy of ionization shows a high stability and thus a chemical inertness, while the low energy of ionization indicates a tendency of the molecule to reactivity. The electronic affinity (A) is characterized as the energy generated by adding an electron to a neutral molecule and thus the high (A) value indicates the molecule tendencies to retain its electrons. A negative chemical potential means that the molecule is extremely stable or can barely decay into its components. The hardness represents the resistance of the molecule electron cloud to be deformed under a small experimental press. A broad HOMO–LUMO energy gap indicates a polar, active, and hard molecule, whereas a narrow HOMO–LUMO energy gap indicates a less polar, less active, and soft molecule. The global electrophilicity (ω) corresponds to the stability energy of a molecule after the addition of external electronic charge[28]. From table 4, the calculated values of ionization potential, electron affinity, chemical potential, electronegativity, hardness, softness and electrophilicity were 4.055, 1.001, -2.528, 2.528, 1.527, 0.654 and 2.092eV, respectively.

Table 4. Global reactivity indices of TTPA-TTF

Parameters	Values
Ionization potential (I) (eV)	4.055
Electron affinity (A) (eV)	1.001
Electronegativity (χ) (eV)	2.528
Electrochemical potential (μ) (eV)	-2.528
Global chemical hardness (η) (eV)	1.527
Global chemical softness (S) (eV^{-1})	0.654
Electrophilicity index (ω) (eV)	2.092

3.7. Bond orbital analysis

The NBO study is a valid tool for evaluating a molecule's charge transfer properties as well as its intramolecular and intermolecular bonding nature. The π electron delocalization means that the occupancy of a certain Lewis valence orbital (donor) decreases as the electron density shifts to another part of the molecule (acceptor). This influence is consistent with certain energy reductions, according to the applied second-order perturbation principle. The strength of delocalization interaction or stabilization energy (E(2)) associated with electron transfer between the donor and acceptor parts can be described as the second-order energy lowering for each donor (i) and acceptor (j) [41-42].

$$E^{(2)} = -q_{ij}\frac{(F_{ij})^2}{\varepsilon_i - \varepsilon_j} \qquad (8)$$

Here, qi is the donor orbital occupancy; and are the orbital energies of donor and acceptor NBO orbitals, respectively; F_{ij} is the off-diagonal Fock or Kohn–Sham matrix element.

The data extracted from the second-order perturbation theory analysis of the Fock matrix of TTPA-TTF are presented in Table 5. The natural Bond Orbital (NBO) analysis of the title molecule suggest that the most important interaction is mainly confined between the benzene rings and lone pair electrons of oxygen and nitrogen atoms. The lone pair of oxygen has the greatest interaction energy contribution in their Lp(n) to π∗ orbitals, because the highest stabilization energies (E (2)) 30.13, 30.21, 30.09, 30.15, 30.04, 30.26, 30.22 et 30.15 kcal/mol were calculated for the transition between LP(2) O1→π*(C14–C15), LP (2)O2→π*(C20–C21), LP(2) O3→π*(C34–C35), LP(2) O4→π*(C41–C42), LP(2) O5→ π*(C56–C57), LP (2) O6→π*(C62–C63), LP(2) O7→π*(C76–C77), LP (2) O8→π*(C82–C83) respectively.

The interactions between Lp (N) and π∗ orbitals are also important in the following cases, LP (1) N1→ π*(C8–C9)(27.89 kcal/mol), LP (1) N2→π*(C27–C28) (26.93 kcal/mol), LP (1) N3→π* (C50–C51) (26.40 Kcal/mol), LP(1)N4→π* (C70–C71) (25.36) kcal/mol). In addition, a significant energy transfer is observed in the Lp (S) and π∗ orbital interactions such that

the stabilization energies are 18.96, 18.75, 19.01 and 18.98 kcal/mol for LP (2) S1 →π *(C2– C4), LP (2) S2 → π *(C3 – C4), LP (2) S3 → π *(C46 – C45), LP (2) S4 →π *(C1 – C2) respectively.

In the TTPA-TTF compound, the π→ π∗ transition of all C–C bonds in a benzene ring has higher stabilization energies associated with them and they give more stability and less reactive to the benzene rings. The range of transition energy between C–C and C–C bonds is 12.68 to 22.79 kcal/mol (e.g. π(C65–C64)→π*(C62–C63)=12.68 kcal/mol,π(C9–C8)→π*(C5–C10)=22.79 kcal/mol, etc.) in the benzene, which indicates that the greater electron density (ED) distribution around the rings.

3.8. NLO properties

The NLO properties of any material generated by the interactions of its electromagnetic fields in different media are important to understand [43]. Indeed, in signal processing, optical switches, networking technology and optical memory modules, NLO compounds are used. The electrical characteristics of the entire molecule influence the linear and nonlinear responses of NLO materials [44]. Hence, Properties, such as the dipole moment (μ), polarizability (αij) and first hyperpolarizability (βtot), are related to non-linear optical properties. In the analysis of organic materials with NLO, this DFT approach has already proven effective. We have summarized our results in Table 6. The complete equations for calculating the value of the total dipole moment (μ_{tot}), the average isotropic polarizability (<α>), the anisotropy of the polarizability Δα and the first order of the hyperpolarizability (βtot), respectively, are the following [45]:

$$\mu_{tot} = \sqrt{\mu_x^2 + \mu_y^2 + \mu_z^2} \quad (9)$$

$$\alpha = \frac{1}{3}\left(\alpha_{xx} + \alpha_{yy} + \alpha_{zz}\right) \quad (10)$$

$$\Delta\alpha = \sqrt{\frac{\left(\alpha_{xx} - \alpha_{yy}\right)^2 + \left(\alpha_{yy} - \alpha_{xx}\right)^2 + \left(\alpha_{zz} - \alpha_{xx}\right)^2}{2}} \quad (11)$$

$$\beta_{tot} = \sqrt{\beta_x^2 + \beta_y^2 + \beta_z^2} \quad (12)$$

Here, $\beta_i = (i = x, y, z)$ combines the different quantities: $\beta_i = (\frac{1}{3})\Sigma_{j=x,y,z}(\beta_{ijj} + \beta_{jij} + \beta_{jji})$

Table 5. Numerical NBO results derived from the second-order perturbation theory analysis of the Fock matrix for TTPA-TTF

Donor (i)	Acceptor (j)	E(2) kcal/mol	E(j)-(i) a.u	F (i.j) a.u	Donor (i)	Acceptor (j)	E(2) kcal/mol	E(j)-(i) a.u	F (i.j) a.u
π (C3–C4)	π* (C25–C26)	4.47	0.93	0.048	π (C46–C45)	π* (C67–C72)	5.24	0.32	0.040
π (C25–C26)	π* (C3–C4)	7.73	0.27	0.042	π (C67–C72)	π* (C46–C45)	8.98	0.28	0.063
π (C25–C26)	π* (C27–C28)	19.10	0.0.27	0.065	π (C46–C45)	π* (C47–C52)	5.04	0.32	0.039
π (C27–C28)	π* (C25–C26)	22.44	0.28	0.072	π (C47–C52)	π* (C46–C45)	16.40	0.28	0.039
π (C25–C26)	π* (C30–C29)	17.15	0.28	0.064	π (C67–C72)	π* (C71–C70)	19.34	0.27	0.066
π (C30–C29)	π* (C25–C26)	20.30	0.28	0.064	π (C71–C70)	π* (C67–C72)	22.32	0.28	0.072
π (C27–C28)	π* (C30–C29)	22.83	0.31	0.076	π (C71–C70)	π* (C68–C69)	17.44	0.29	0.064
π (C30–C29)	π* (C27–C28)	17.34	0.29	0.064	π (C68–C69)	π* (C71–C70)	20.28	0.28	0.067
π (C31–C36)	π* (C35–C34)	17.60	0.28	0.064	π (C67–C72)	π* (C68–C69)	20.67	0.28	0.069
π (C35–C34)	π* (C31–C36)	21.55	0.29	0.071	π (C68–C69)	π* (C67–C72)	17.19	0.28	0.069
π (C31–C36)	π* (C32–C33)	20.38	0.29	0.069	π (C80–C81)	π* (C82–C83)	20.75	0.31	0.073
π (C32–C33)	π* (C31–C36)	17.53	0.28	0.064	π (C82–C83)	π* (C80–C81)	22.09	0.32	0.076
π (C35–C34)	π* (C32–C33)	17.40	0.29	0.064	π (C80–C81)	π* (C85–C84)	20.35	0.29	0.068
π (C32–C33)	π* (C35–C34)	20.39	0.28	0.069	π (C85–C84)	π* (C80–C81)	20.81	0.31	0.074
π (C38–C43)	π* (C42–C41)	20.42	0.29	0.031	π (C82–C83)	π* (C85–C84)	21.34	0.32	0.074
π (C42–C41)	π* (C38–C43)	17.63	0.28	0.073	π (C85–C84)	π* (C82–C83)	21.43	0.31	0.074
π (C38–C43)	π* (C39–C40)	17.67	0.28	0.064	π (C73–C78)	π* (C77–C76)	22.28	0.32	0.075

π (C39–C40)	π* (C38–C43)	21.54	0.29	0.071	π (C77–C76)	π* (C73–C78)	20.95	0.31	0.075
π (C42–C41)	π* (C39–C40)	17.42	0.29	0.071	π (C73–C78)	π* (C74–C75)	20.58	0.31	0.072
π (C39–C40)	π* (C42–C41)	20.47	0.28	0.069	π (C74–C75)	π* (C73–C78)	22.93	0.32	0.073
π (C3–C4)	π* (C5–C10)	5.08	0.0.32	0.039	π (C74–C75)	π* (C77–C76)	20.83	0.32	0.073
π (C5–C10)	π* (C3–C4)	8.90	0.27	0.045	π (C77–C76)	π* (C74–C75)	21.75	0.31	0.075
π (C5–C10)	π* (C6–C7)	20.96	0.28	0.045	π (C47–C52)	π* (C51–C50)	21.72	0.31	0.075
π (C6–C7)	π* (C5–C10)	16.78	0.28	0.063	π (C51–C50)	π* (C47–C52)	19.54	0.31	0.071
π (C5–C10)	π* (C9–C8)	20.41	0.28	0.069	π (C47–C52)	π* (C48–49)	20.85	0.31	0.072
π (C9–C8)	π* (C5–C10)	22.79	0.32	0.078	π (C48–49)	π* (C47–C52)	22.67	0.32	0.077
π (C6–C7)	π* (C9–C8)	20.41	0.28	0.069	π (C48–49)	π* (C51–C50)	22.86	0.31	0.077
π (C9–C8)	π* (C6–C7)	17.60	0.29	0.064	π (C51–C50)	π* (C48–49)	19.50	0.32	0.072
π (C18–C19)	π* (C20–C21)	20.86	0.29	0.069	π (C60–C61)	π* (C62–C63)	13.52	0.31	0.058
π (C20–C21)	π (C18–C19)	20.89	0.31	0.074	π (C62–C63)	π* (C60–C61)	12.89	0.32	0.059
π (C18–C19)	π* (C22–C23)	17.55	0.28	0.064	π (C60–C61)	π* (C65–C64)	20.00	0.31	0.072
π (C22–C23)	π* (C18–C19)	21.61	0.29	0.064	π (C65–C64)	π* (C60–C61)	21.99	0.32	0.076
π (C20–C21)	π* (C22–C23)	20.42	0.28	0.064	π (C65–C64)	π* (C62–C63)	12.68	0.31	0.057
π (C22–C23)	π* (C20–C21)	17.36	0.29	0.064	π (C62–C63)	π*(C65–C64)	13.35	0.31	0.060
π (C11–C16)	π* (C14–C15)	17.64	0.028	0.064	π (C53–C58)	π* (C57–C56)	22.17	0.32	0.075
π (C14–C15)	π* (C11–C16)	21.59	0.29	0.071	π (C57–C56)	π* (C53–C58)	20.68	0.31	0.074
π (C11–C16)	π* (C12–C13)	20.44	0.29	0.096	π (C53–C58)	π* (C54–C55)	20.73	0.31	0.073
π (C12–C13)	π* (C11–C16)	17.63	0.28	0.064	π (C54–C55)	π* (C53–C58)	20.68	0.31	0.074
π (C14–C15)	π* (C12–C13)	17.40	0.29	0.064	π (C54–C55)	π* (C57–C56)	21.44	0.31	0.074
π (C12–C13)	π* (C14–C15)	20.50	0.28	0.069	π (C57–C56)	π* (C54–C55)	21.15	0.32	0.076
LP (2) S1	π* (C1–C2)	15.53	0.26	0.060	LP (2) S3	π* (C 3–C4)	18.96	0.27	0.065
LP (2) S1	π* (C46–C45)	19.01	0.27	0.065	LP (2) S3	π* (C1–C2)	15.49	0.26	0.060
LP (2) S2	π* (C1–C2)	18.98	0.24	0.064	LP (2) S4	π* (C3–C4)	18.75	0.26	0.058
LP (2) S2	π* (C46–C45)	15.33	0.26	0.058	LP (2) S4	π* (C1–C2)	15.76	0.24	0.064
LP (1) N1	π* (C8–C9)	27.89	0.27	0.080	LP (1) N4	π* (C73–C78)	15.20	0.27	0.059
LP (1) N1	π* (C18–C19)	15.39	0.27	0.059	LP (1) N4	π* (C70–C71)	25.36	0.27	0.076
LP (1) N1	π* (C11–C16)	15.68	0.27	0.060	LP (1) N4	π* (C80–C81)	17.30	0.27	0.063
LP (1) N2	π* (C27–C28)	26.93	0.27	0.079	LP (1) N3	π* (C53–C58)	16.61	0.27	0.061
LP (1) N2	π* (C38–C43)	15.89	0.27	0.060	LP (1) N3	π* (C60–C61)	15.39	0.27	0.059
LP (1) N2	π* (C31–C36)	15.65	0.27	0.060	LP (1) N3	π* (C50–C51)	26.40	0.27	0.073
LP (2) O1	π* (C14–C15)	30.13	0.34	0.096	LP (2) O5	π* (C56–C57)	30.04	0.34	0.96
LP (2) O2	π* (C20–C21)	30.21	0.34	0.096	LP (2) O6	π* (C62–C63)	30.26	0.34	0.096
LP (2) O3	π* (C34–C35)	30.09	0.34	0.096	LP (2) O7	π* (C76–C77)	30.22	0.34	0.096
LP (2) O4	π* (C41–C42)	30.15	0.34	0.096	LP (2) O8	π* (C82–C83)	30.15	0.34	0.096

4. Conclusion

In this paper, we study through DFT/B3LYP/6-31G(d) calculations the geometrical and electron-ic structure of the TTPA-TTF compound. The molecular geometry was optimized at the B3LYP/ 6-31G(d) level of theory in the gas phase. The dihedral angles between the oriented TTF and the peripheral TPA groups for TTPA-TTF were in the range of 45°- 47°, suggesting that the compound had a twisted structure. The par-tial atomic charge distribution study showed a concentration of negative charge on the nitrogen, oxygen, and sulfur

atoms, while the carbon at-oms of the tetrathiafulvalene unit are clearly positively charged. According to an analysis of the molecular orbital topology, there is a 3.055 eV energy difference between the HOMO and LUMO orbitals. this gap suggests that an intramo-lecular charge transfer (ICT) from the TTF unit to the adjacent phenyl.

The MESP map shows clearly the most negative area surrounding the TTF unit and oxygen atom, as this region is extremely prone to electrophilic attack. on the contrary, hydrogen atoms seem to be among the most positively charged, making them ideal targets for nucleophilic attack. The basic chemical reactivity descriptors were com-puted, implying that the TTPA-TTF compound is a reasonably soft molecule with high polarizabil-ity and chemical activity. Finally, the calculated non-linear optical properties validated the TTPA-TTF compound's ability as a good NLO material.

References

[1] S. M. Rosenfeld, R. G. Lawlert and H. R. Ward, Electron Transfer in a New Highly Conducting Donor-Acceptor Complex, J. Am. Chem. Soc. 837 (1973) 948–949.

[2] S. Rabaça, S. Oliveira, A. Cláudia, D. Simão, I. Cordeiro, M. Almeida, CyanobenzeneTTF-type donors; synthesis and characterization, J. Tetrahedron Letters. 55(2014) 6992–6997.

[3] V. A. Azov, Recent advances in molecular recognition with tetrathiafulvalene-based receptors, J. Tetrahedron Lett. 57(2016) 5416-5425.

[4] N. Martín, Tetrathiafulvalene: The advent of organic metals, J. Chem. Commun, 49(2013) 7025–7027.

[5] M. R. Bryce, Functionalised tetrathiafulvalenes: New applications as versatile π- electron systems in materials chemistry, J. Mater. Chem. 10(2000)589–598.

[6] J. L. Segura, N. Martn, New concepts in tetrathiafulvalene chemistry, J. Angew. Chemie - Int. Ed. 40(2001)1372–1409.

[7] M. B. Nielsen, C. Lomholt, J. Becher, Tetrathiafulvalenes as building blocks in supramolecular chemistry II, J. Chem. Soc. Rev, 29 (2000) 153–164.

[8] M. Sallé, D. Zhang, D. Canevet, M. Salle, Tetrathiafulvalene (TTF) derivatives : key building-blocks for switchable processes, J. Chem. Commun.7345(2009)2245-2269

[9] E. Laukhina, V. Laukhin, and J. Veciana, Multistability in a BEDT-TTF Based Molecular Conductor, J. Am. Chem. Soc.125 (2003) 3948–3953.

[10] L. Martin, Molecular conductors of BEDT-TTF with tris (oxalato) metallate anions, J. Coordination Chemistry. 376 (2018) 277-291.

[11] N. Martín, D. M. Guldi, Stabilisation of charge-separated states via gain of aromaticity and planarity of the donor moiety in C 60 -based dyads, J. Chemical Communications. (2000) 113–114.

[12] J. Roncali, Linearly extended p -donors : when tetrathiafulvalene meets conjugated oligomers and polymers, J. Mater. Chem. 7 (1997) 2307–2321.

[13] A. Ayadi, TTF based donor-pi-acceptor dyads synthesized for NLO applications, J. Dye. Pigment. 138 (2016) 255-266.

[14] T. K. Hansen, T. Jprrgensen, P. C. Stein, J. Becher, Crown Ether Derivatives of Tetrathiafulvalene . 1, J. Org. Chem. 57 (1992) 6403–6409.

[15] C. Gime and C. J. Go, Hybrid Organic/Inorganic Molecular Materials Formed by Tetrathiafulvalene Radicals and Magnetic Trimeric Clusters of Dimetallic Oxalate-Bridged Complexes: The Series (TTF)4{MII(H2O)2[MIII(ox)3]2}·nH2O (MII = Mn, Fe, Co, Ni, Cu and Zn; MIII = Cr and Fe; ox = C2O42−), Eur. J. Inorg. Chem. 2003 (2003) 2290-2298.

[16] H. Ringsdorf, H. Bengs, O. Karthaus, R. Wüstefeld, M.Ebert, J.H. Wendorff, B, Kohne, K.Praefcke, Induction and Variation of Discotic Columnar Phases through Doping with Electron Acceptors, J. Advanced materials. 2 (1990) 141–144.

[17] M. R. Bryce, W. Devonport, L. M.

Goldenberg, C. Wang, Macromolecular tetrathiafulvalene chemistry, J. Chem. Commun. (1998) 945–951.

[18] M. Asakawa, A Chemically and Electrochemically Switchable [2]Catenane Incorporating a Tetrathiafulvalene Unit, J. Angew. Chem. Int. Ed. 37 (1998) 333–337.

[19] P. W. Thulstrup, S. V. Hoffmann, N. C. Jones, J. Spanget-Larsen, Electronic transitions of tetrathiafulvalene oriented in polyethylene film - Near and vacuum UV synchrotron radiation polarization spectroscopy, J. Chem. Phys. Impact. 2 (2020) 2-21.

[20] X.Tian, F. QianMin, W. Liang, F. Zhang,D.Li,K. Guo, Z. Liu, J. Li, Synthesis and properties of triphenylamine functionalized tetrathiafulvalene, J. Tetrahedron Lett. 61 (2020) 1-4.

[21] X. Liu A star-shaped carbazole-based hole-transporting material with triphenylamine side arms for perovskite solar cells, J. Mater. Chem. 6 (2018) 12912–12918.

[22] J. Wang, K. Liu, L. Ma, X. Zhan, Triarylamine: Versatile Platform for Organic, Dye-Sensitized, and Perovskite Solar Cells, J. Chem. Rev. 116 (2016) 14675–14725.

[23] R. Yuan Design, synthesis and photoelectrical properties of diphenylamine-containing triphenylamine-based D-D-π-A-type fluorescence dyes, J. Tetrahedron Lett. 60 (2019) 1803–1807.

[24] A. D. Becke, Density-functional exchange-energy approximation with correct asymptotic behavior, J. Phys. Rev. A. 38 (1988) 3098-3100

[25] C. J. Frisch, G. W. Trucks, H. B. Schlegel, G. E .Scuseria, M. A. Robb et al. (2009) Gaussian 09, Revision A.02.

[26] P. Geerlings F. De Proft, Conceptual DFT: The chemical relevance of higher response functions, J. Phys. Chem. Chem. Phys. 10 (2008) 3028–3042.

[27] P. W. Ayers, J. S. M. Anderson, L. J. Bartolotti, Perturbative perspectives on the chemical reaction prediction problem, J. Int. J. Quantum Chem. 101 (2005) 520–534.

[28] R. G. Parr, C. Hill, N. Carolina, Electrophilicity Index,J. Am. Chem. Soc. 121 (1999) 1922–1924.

[29] J. Tirado-Rives, W. L. Jorgensen, Performance of B3LYP density functional methods for a large set of organic molecules, J. Chem. Theory Comput.4 (2008) 297–306.

[30] M. M. C. Ferreira, E. Suto, Atomic Polar Tensor Transferablity and Atomic Charges kr the Fluoromethane Series CHxF4-x, J. Phys. Chem. 96 (1992) 8844–8849.

[31] F. J. Luque, J. M. López, M. Orozco, Perspective on "Electrostatic interactions of a solute with a continuum. A direct utilization of ab initio molecular potentials for the prevision of solvent effects", J. Theor. Chem. Acc., 103 (2000) 343–345.

[32] G. Gogoi, S. R. Sahoo, B. K. Rajbongshi, S. Sahu, N. Sen Sarma, S. Sharma, New types of organic semiconductors based on diketopyrrolopyrroles and 2,1,3-benzochalcogenadiazoles: a computational study, J. Mol. Model. 25 (2019) 1-12.

[33] S. R. Kumar, N. Vijay, K. Amarendra, P. Onkar, S. Leena, Theoretical Studies on the Isomers of Quinazolinone by first Principles, J. Res.J.Recent Sci. 1 (2012) 11–18.

[34] A. Dreuw, M. Head-Gordon, Failure of Time-Dependent Density Functional Theory for Long-Range Charge-Transfer Excited States: The Zincbacteriochlorin−Bacteriochlorin and, J. Am. Chem. Soc. 126 (2004) 4007–4016.

[35] Z. L. Zhang, L. Y. Zou, A. M. Ren, Y. F. Liu, J. K. Feng, C. C. Sun, Theoretical studies on the electronic structures and optical properties of star-shaped triazatruxene/heterofluorene co-polymers, J. Dye. Pigment. 96 (2013) 349–363.

[36] G. Scalmani, M. J. Frisch, B. Mennucci, J. Tomasi, R. Cammi, V. Barone, Geometries

and properties of excited states in the gas phase and in solution: Theory and application of a timedependent density functional theory polarizable continuum model, J. Chem. Phys. 124 (2006) 094-107.

[37] S. K. Lanke and N. Sekar, Rigid Coumarins: A Complete DFT, TD-DFT and Non Linear Optical Property Study, Journal of Fluorescence. 25 (2015) 1469–1480.

[38] T. Koopmans, Über die Zuordnung von Wellenfunktionen und Eigenwerten zu den Einzelnen Elektronen Eines Atoms, J. Physica. 1 (1934) 104–113.

[39] Z. Zhou, R. G. Parr, New Measures of Aromaticity: Absolute Hardness and Relative Hardness, *J. Am. Chem. Soc.* 111 (1989) 7371–7379.

[40] R. G. Parr, R. G. Pearson, Absolute Hardness : Companion Parameter to Absolute Electronegativity, J. Am. Chem. SOC. 105 (1983) 7512–7516.

[41] M. Thirunavukkarasu , G. Balaji , S. Muthu , B R. Raajaraman , P. Ramesh, Computational spectroscopic investigations on structural validation with IR and Raman experimental evidence, projection of ultraviolet-visible excitations, natural bond orbital interpretations, and molecular docking studies under the biological investigation on N-Benzyloxycarbonyl-L-Aspartic acid 1-Benzyl ester, J. Chemical Data Collections. 31 (2021) 100622

[42] A. E. REED, L. A. CURTISS, F. WEINHOLD, Intermolecular Interactions from a Natural Bond Orbital, Donor-Acceptor Viewpoint, J. Chem. Rev. 88 (1988) 899-926

[43] M. Bourass, A. El Alamy, and M. Bouachrine, Comptes Rendus Chimie Structural and photophysical studies of triphenylamine-based nonlinear optical dyes : effects of p -linker moieties on the D-p -A structure, J. Comptes rendus - Chim., 22 (2019) 373–385.

[44] M. Khalid , A. Ali, R. Jawaria, M. A. Asghar, S. Asim, M. U. Khan, R. Hussain, M. F. Rehman, C. J. Ennis, M. S. Akram, First principles study of electronic and nonlinear optical properties of A – D – p – A and D – A – D – p – A con fi gured compounds containing novel, J. RSC Adv. 10 (2020) 22273–22283.

[45] A. Alparone, Static and Dynamic Electronic (Hyper)polarizabilities of Dimethylnaphthalene Isomers: Characterization of Spatial Contributions by Density Analysis, J. Research Article. 2013 (2013) 1-9.